

## Generating Tactile Afferent Stimulation Patterns for Slip and Touch Feedback in Neural Prosthetics

Danielle M. Rager, *Student Member IEEE*, Darren Alvares, *Student Member IEEE*, Ingvars Birznieks, Stephen J. Redmond, *Member IEEE*, John W. Morley, Nigel H. Lovell, *Fellow IEEE*, Richard M. Vickery

**Abstract**— Current prosthetic limbs are limited by a lack of tactile feedback. Slip feedback is particularly important to inform grip. Object slip is marked by both a change in the normal grip force applied and a change in force tangential to the fingertips. In this study, we demonstrate that a new multi-axial tactile sensor composed of gold nanoparticle strain gauges is able to record slip and reconstruct the X, Y, and Z forces incident on the sensor's surface due to a slipping object. We entered the X, Y, and Z force components generated by the slip event into a noisy leaky integrate and fire model to simulate the firing responses of SA1 and FA1 afferents. We also recorded a uniaxial normal force input representative of tactile contact. A single set of SA1 model and FA1 model parameters generated realistic firing patterns for both the slip and normal force recordings. These results suggest that canonical SA1 and FA1 afferent models could be used to generate biomimetic electrical stimulation patterns for both slip and touch stimuli. When used to activate the tactile afferents of an amputee, these electrical stimulation patterns could create natural and distinguishable slip and touch percepts for closed loop control of an upper limb neural prosthesis.

### I. INTRODUCTION

Tactile input is essential for successful object manipulation [1]. A delicate task like gripping an egg requires a person to apply a force sufficiently small enough to avoid crushing the egg, but great enough that the egg does not slip. A person must receive feedback from the peripheral nervous system about the grip force they are applying and, in the instance of slip, information about the changing frictional force between the slipping object and the surface of the fingertips.

In an able-bodied human, tactile receptors embedded in the skin of the hand detect tactile stimuli and transmit the information to the central nervous system via their adjoined tactile afferents [2]. While upper limb amputees have been helped by prosthetic limbs, only a few prototypes have

attempted to incorporate tactile sensory feedback systems to inform internal motor control loops of the prosthesis and conscious perception of tactile stimuli [3–6]. Recent advances in neurally-controlled prosthetic limb technology have allowed humans to execute prosthetic hand movements involving the articulation of single fingers [7], but the incorporation of sensory feedback for closed-loop control remains the most challenging task. One proposed method of providing sensory feedback to users of an upper limb neural prosthesis is to outfit the prosthetic hand with tactile sensors and convert the output of these sensors to an electrical stimulation pattern used to activate the user's remaining tactile afferents in the upper arm. The purpose of this paper is to translate continuous, analog slip and contact signals from a sensor into a neural code consisting of a discrete series of action potentials, or “spikes”, that evoke the appropriate percept.

Prior research on tactile feedback has been limited by the need for a lightweight tactile sensor with good response bandwidth and, in the case of slip detection, sensitivity to shear forces [8]. We propose the use of a new sensor composed of four gold nanoparticle (AuNP) strain gauges [9], [10]. In this sensor, differences in the relative change in resistance of the four sensing units can be used to determine the direction of an applied force. This feature allows the sensor to distinguish shear force from normal force, and therefore, differentiate a slip stimulus from a normal force stimulus. We believe that the sensor's response to slip and touch could be used to create two distinguishable signals in users of neural prosthetics.

Tactile percepts are dependent on both the spiking pattern of tactile afferents and the type of tactile afferents activated. Human glabrous skin has four types of low-threshold tactile afferents essential for control of the hand [1]. We will initially focus on two of those which, when selectively activated, may recreate differentiable percepts for slip and touch [11]. These two types of afferents are slowly adapting type I afferents (SAIs), which respond to local pressure sensations, and rapidly adapting type I afferents (FAIs), which respond primarily to changes in pressure [2].

To generate physiological neural codes for FAIs and SAIs, the AuNP sensor's outputs were entered into two variations of an integrate and fire (IF) model, a mathematical model used to predict neuronal spiking [12]. Each of the IF models predicted the firing pattern of a single tactile afferent type. For a given afferent type, one canonical set of IF parameters (tuned using a real neural data set) generated physiologically realistic firing patterns for the sensor responses to both slip and touch stimuli. These predicted

\*Research supported by Whitaker International and the ARC Thinking

D. M. Rager is with the School of Physiology, University of New South Wales (UNSW), Kensington, NSW, 2052, AUS. (phone: 0406-061-140, email: d.rager@student.unsw.edu.au)

D. Alvares is with the Graduate School of Biomedical Engineering, UNSW. (email: d.alvares@student.unsw.edu.au)

I. Birznieks is with Neuroscience Research Australia, Randwick, NSW, 2031, AUS and the School of Medical Science, University of Western Sydney (UWS), Campbelltown, NSW, 2560, AUS. (email: i.birznieks@neura.edu.au)

S. J. Redmond is with the Graduate School of Biomedical Engineering, UNSW. (email: s.redmond@unsw.edu.au)

J.W. Morley is with the School of Medical Science, UWS. (email: j.morley@uws.edu.au)

N.H. Lovell is with the Graduate School of Biomedical Engineering, UNSW. (email: n.lovell@unsw.edu.au)

R. M. Vickery is with the School of Physiology, UNSW. (email: richard.vickery@unsw.edu.au)

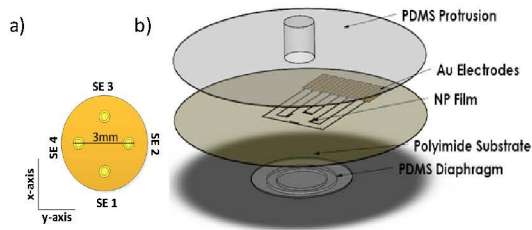


Fig. 1: a) Diagram of the multi-axial tactile sensor. b) Top-view of the sensor's axisymmetric sensing element configuration.

firing patterns could be converted to current pulse trains used to activate the targeted afferent type, creating the distinguishable percepts for touch and slip necessary for grip feedback.

## II. SENSOR MEASUREMENTS

In this study, the tactile sensor used consisted of a polydimethylsiloxane (PDMS) protrusion to which force was applied and of an underlying array of four sensing AuNP strain gauges. These strain gauges, along with a reference gauge, are printed on a plastic polyimide substrate (Fig. 1, a, b). For NP film strain gauge sensors, the resistance of a gauge increases when positive strain is applied to the film and decreases when negative strain is applied [13]. A shear force applied to the sensor protrusion will result in negative strain on the gauge nearest the force applied and positive strain on the gauge directly opposite the force applied. Using this principle, the sensor can detect the direction of force applied along an axis. The reference gauge, which is located on the portion of the sensor that is not subject to any force, is used to adjust for temperature effects.

The sensor's response to slip and touch was tested using a DC3K micromanipulator (Marzhauser Wetzlar, Germany) and an AFG force gauge (Mecmesin, UK). Sensor output is measured using a current loop circuit [14] and an NI-DAQ system. For touch trials, a probe tip attached to the micromanipulator applied additional normal force to the top of the sensor protrusion. (A baseline normal force of 120 mN was used to hold the sensor in place.) For slip trials, a probe tip with a wide, flat surface exerted a normal force onto the sensor protrusion. The micromanipulator drove the probe tip on the XY plane, tangential to the protrusion surface (Fig. 2). When the shear force exerted by the probe exceeded the traction, the probe tip slipped across the surface of the protrusion. Five channels of data were sampled at 1 kHz: four for the outputs of the strain gauges of the sensor, and one for the force gauge. The voltage measurements from the force gauge were converted to force measurements using preliminary calibration data, in which the analog voltage output was regressed against the digital force value displayed on the force gauge's screen during a series of normal force applications.

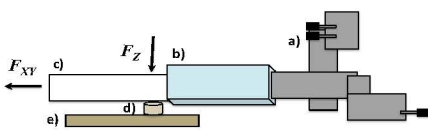


Fig. 2: Setup for slip trials a) Micromanipulator b) force gauge c) probe tip d) PDMS protrusion e) NP film in polyimide substrate

The voltage measurements from the four sensing strain gauges were converted back into relative change in resistance values using the current and resistance values of the current loop circuit. The relative change in resistance of the four sensing units can be related to the force applied using (1),

$$F = AR \quad (1)$$

where  $F$  is a  $3 \times 1$  vector containing  $[F_x, F_y, F_z]$ ,  $R$  is  $4 \times 1$  vector containing  $\Delta R/R$ , the relative change resistance of each strain gauge, and  $A$  is  $3 \times 4$  calibration matrix. Assuming orthogonality of the three force axes and identical sensitivity of the four strain gauges, (1) can be reduced to (2), which comprises three simple linear regression problems, where  $X_s$ ,  $Y_s$ , and  $Z_s$  are the calculated sensitivities in the X, Y, and Z directions, respectively.

$$\begin{aligned} F_x &= \left( \frac{\Delta R_3}{R_3} - \frac{\Delta R_1}{R_1} \right) / X_s \\ F_y &= \left( \frac{\Delta R_2}{R_2} - \frac{\Delta R_4}{R_4} \right) / Y_s \\ F_z &= \left( \frac{\Delta R_1}{R_1} + \frac{\Delta R_2}{R_2} + \frac{\Delta R_3}{R_3} + \frac{\Delta R_4}{R_4} \right) / Z_s \end{aligned} \quad (2)$$

Assuming identical sensitivity of the four strain gauges, we were able to reconstruct  $\Theta$ , the angle of the force in the XY plane using (3),

$$\Theta = \tan^{-1} \left( \left( \frac{\Delta R_2}{R_2} - \frac{\Delta R_4}{R_4} \right) / \left( \frac{\Delta R_3}{R_3} - \frac{\Delta R_1}{R_1} \right) \right) \quad (3)$$

The relative change in resistance values were then regressed against the X and Y components of force as described in (2). Though the force gauge was only capable of measuring uniaxial force and was set to measure the force applied in the XY plane, normal force could be reconstructed using the frictional force equation (4),

$$F_z \cdot \mu_s = F_{XY} \quad (4)$$

where  $\mu_s$  is the coefficient of static friction of the thermoplastic probe tip against the PDMS protrusion, and  $F_{XY}$  is the force applied in the XY plane. The value of  $\mu_s$  was estimated to 1 based on previous studies of the coefficient of static friction of PDMS against hydrophobic surfaces such as thermoplastic [15]. The relative change in resistance of all four strain gauges was regressed against the approximated normal force to calculate  $Z_s$ , as described in (2).

## III. TACTILE AFFERENT MODELS

We aimed to convert the force vector  $F$  into biomimetic tactile afferent firing patterns that would elicit an appropriate percept in a prosthetic limb user. Able-bodied humans encode slip and touch stimuli primarily with SA1s, which respond to local pressure sensations, and FA1s, which transmit information on edges and vibrations from 20-100 Hz [1]. SA1s are slowly adapting because they remain active during static stimuli and are slow to return to a baseline firing rate. Likewise, FA1s are rapidly adapting because they respond primarily to changes in stimuli and rapidly return to a baseline firing rate in response to static stimuli. Given the adaptation characteristics of the two afferent types, firing patterns that emulate those of an SA1 afferent result from a neuronal model that emphasizes force input signals, while firing patterns that emulate those of an FA1 afferent are more dependent on force derivative input signals [16], [18].

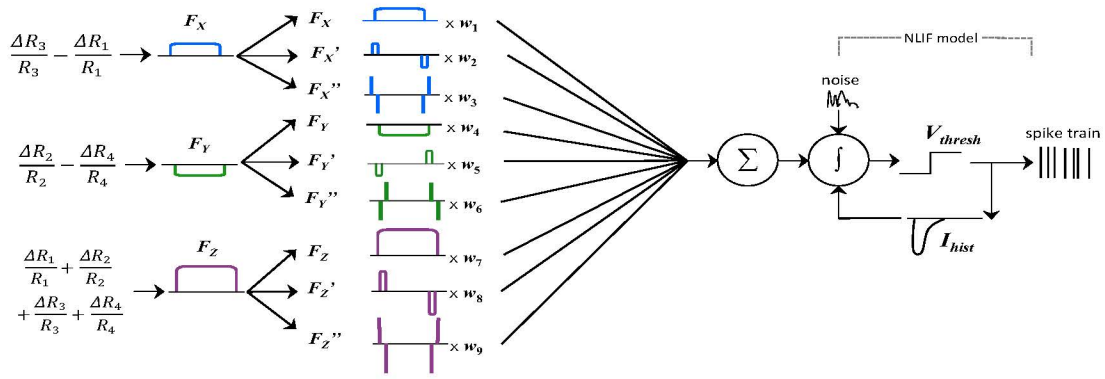


Fig. 3: System diagram of a tactile afferent model. Relative changes in resistance of the four sensing units are converted to forces in the X, Y, and Z directions. These force signals are differentiated with respect to time, multiplied by a weight constant, and summed to create the input to a noisy leaky integrate and fire model. Weight constants are adjusted differently to create a model that emulates SA1 afferents, which are primarily sensitive to force, and a model that emulates FA1 afferents, which are primarily sensitive to changes in force over time.

A weighted sum of  $F_X$ ,  $F_Y$ , and  $F_Z$ , their derivatives ( $F_X'$ ,  $F_Y'$ ,  $F_Z'$ ), and second derivatives ( $F_X''$ ,  $F_Y''$ ,  $F_Z''$ ) with respect to time were entered into a variation of an IF model, which predicts the times at which a neuron fires. Force derivative signals were computed using a fourth order Savitzky-Golay filter with a frame size of five samples to smooth the data and avoid noise amplification due to differentiation [17]. Derivative signals were zero-padded to match the length of the original force signal.

The weighted sum of the force signals and force signal time derivatives (nine signals in total) served as the input,  $I_{stim}$ , to a noisy leaky integrate and fire model (NLIF), described by (5),

$$dV = \frac{1}{C} (-g(V(t) - V_{leak}) + I_{stim}(t) + I_{hist}(t))dt + W_t \quad (5)$$

where  $V$  is the afferent's membrane potential,  $C$  is the membrane capacitance,  $g$  is the leak conductance,  $V_{leak}$  is the membrane resting potential,  $I_{hist}$  is a post-spike inhibitory current, and  $W_t$  is a Gaussian noise term (Fig. 3). When  $V(t)$  reaches a set threshold value  $V_{thresh}$ , a spike is fired, and  $V(t)$  is reset to a chosen value,  $V_{reset}$ .  $I_{hist}$  is calculated using (6),

$$I_{hist}(t) = \sum_{j=0}^{i-1} h(t - t_j) \quad (6)$$

where  $h$  is the postspike current waveform following the form of a raised cosine basis function [19].  $C$  and  $g$  can be

re-stated in terms of a single variable  $\tau$ , the time constant of the "leaky integrator". In this study,  $V_{reset}$  and  $V_{threshold}$  were fixed parameters set to 0 and 1, respectively, on a normalized voltage scale. The remaining free parameters— $\tau$ ,  $V_{leak}$ ,  $\sigma$  (the standard deviation of  $W_t$ ), all time points of  $h$ , and the nine weights  $w_1$ - $w_9$  for the force signal inputs—were optimized using a standard maximum likelihood estimation (MLE) procedure for NLIF models [19], in which the spike times predicted by the model are optimized to match those of a real neural spike train. Non-human primate FA1 and SA1 responses to torque stimuli from study [20] were used as training data for the MLE algorithm. This training data set contained the necessary  $F_X$ ,  $F_Y$ , and  $F_Z$  force inputs.

#### IV. RESULTS

The NLIF models for an SA1 and FA1 resulted in physiologically realistic spike trains for the slip and touch forces recorded by the sensor. Firing rates from all model outputs did not exceed 300 spikes per second, emulating the known firing behavior of tactile afferents [11]. For touch trials, the FA1 model generated spikes primarily at the onset and termination of force, while the SA1 model remained active throughout the force application but showed increased activation at the stimulus onset and termination (Fig. 4.1). These results are consistent with the established firing

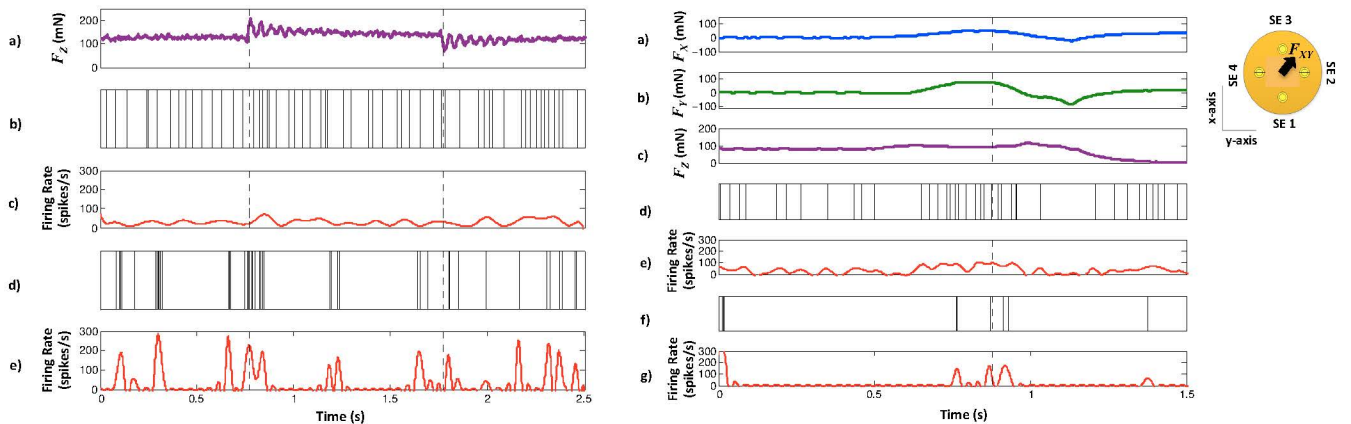


Fig 4.1: Sensor and model outputs to a touch stimulus that compressed the sensor 20  $\mu\text{m}$ . Dotted lines indicate the onset and offset of the added normal force. a) Normal force calculated from sensor response to touch stimulus. b) SA1 model spike train output c) SA1 model output firing rate d) FA1 model spike train output e) FA1 model output firing rate. Fig 4.2: Sensor and model outputs to a slip stimulus. Dotted line indicates slip onset. a-c) X, Y, and Z components of force, respectively, calculated from the sensor response to slip stimulus d) SA1 model spike train output e) SA1 model output firing rate f) FA1 model spike train output g) FA1 model output firing rate.



TABLE I. NLIF AFFERENT MODEL WEIGHTS

	$w_1$	$w_2$	$w_3$	$w_4$	$w_5$	$w_6$
SA1	0.405	8.908	0.382	-0.001	0.001	5.422e-4
FA1	1.417	2.359	0.452	-0.012	-9.912e4	0.024

behaviors of SA1s and FA1s in response to normal forces [2].

The sensor's response to slip had not been tested prior to this study. The sensor was able to detect slip, showing marked change in the direction of force in the X and Y planes (Fig. 4.2). The slip stimulus detected by the sensor was approximately 260 milliseconds in length. The spike trains generated by the FA1 and SA1 models based on these signals are consistent with previous recordings of human SA1 and FA1 afferents [11]. Table 1 shows the trained NLIF model values for  $w_1$ - $w_3$ , the weights for  $F_X$ ,  $F_Y$ , and  $F_Z$  respectively, and  $w_4$ - $w_6$ , the weights for  $F_X'$ ,  $F_Y'$ , and  $F_Z'$ , respectively. The second derivative weights were zeros for both NLIF models.

It should be noted that afferent responses to a stimulus vary even within an SA1 or FA1 population due to different receptor tunings and noise from signal transduction and integration. We have trained SA1 and FA1 NLIF models using data from a single, representative SA1 and FA1 afferent, respectively, to create plausible generic neural responses to a stimulus. Though a generic neural code will not precisely match the temporal activation pattern of every SA1 or FA1, it should be representative of an average response within an afferent population and therefore should allow a prosthetic user to naturally associate the code with its stimulus.

## V. CONCLUSION

The eventual goal of this research is to provide natural feeling tactile feedback to prosthetic limb users. Because slip and touch perception arises primarily from the activation of SA1s and FA1s, targeted electrical stimulation of these afferents in a biomimetic temporal pattern should elicit an instinctive slip or touch percept. Future human stimulation trials will verify whether the temporal spike patterns generated from our NLIF models in response to slip will be perceptually differentiable from the spike patterns generated in response to touch.

The existing protocol does not include an NLIF model for rapidly adapting type II afferents (FA2s), which respond to the onset of stimuli and provide cues to motor programs [1]. This firing behavior may help inform responses to slip stimuli. Though the current study was limited by a lack of FA2 responses to three-dimensional force (which would be needed to tune the parameters of an FA2 NLIF model), we plan to incorporate an FA2 model into our stimulation paradigm in future research.

Successful tactile restoration requires discriminative touch and slip detection for object manipulation. While touch detection is possible with a uniaxial sensor, slip recognition is greatly enhanced by a sensor that can detect changes in shear force along multiple axes. This creates the added challenge of measuring the three-dimensional stress pattern and converting it into a single afferent stimulation pattern. Here, we demonstrated that a novel type of sensor could capture a slip stimulus, reconstruct its  $F_X$ ,  $F_Y$ , and  $F_Z$  force components, and convert those recorded force components to a realistic

spike train using an NLIF model for an SA1 or FA1 afferent, a necessary first step toward restoration of tactile input used for object property exploration and motor control.

## REFERENCES

- [1] R. S. Johansson and J. R. Flanagan, "Coding and use of tactile signals from the fingertips in object manipulation tasks.," *Nature reviews, Neurosci.*, vol. 10, no. 5. pp. 345–59, 2009.
- [2] R. S. Johansson and Å. B. Vallbo, "Tactile sensory coding in the glabrous skin of the human hand," *Trends in Neurosci.*, vol. 6, no. January, pp. 27–32, 1983.
- [3] M. Haugland, a Lickel, J. Haase, and T. Sinkjaer, "Control of FES thumb force using slip information obtained from the cutaneous electroneurogram in quadriplegic man.," *IEEE trans. on Rehab. Eng.*, vol. 7, no. 2. pp. 215–27, 1999.
- [4] G. S. Dhillon and K. W. Horch, "Direct neural sensory feedback and control of a prosthetic arm," *IEEE Trans. on Neural Systems and Rehab. Eng.*, vol. 13, no. 4. pp. 468–472, 2005.
- [5] C. Cipriani, C. Antfolk, C. Balkenius, B. Rosén, G. Lundborg, M. C. Carrozza, and F. Sebelius, "A Novel Concept for a Prosthetic Hand With a Bidirectional Interface: A Feasibility Study," *IEEE Trans. on Biomed. Eng.*, vol. 56, no. 11 Pt 2, pp. 2739–2743, 2009.
- [6] A. Panarese, B. B. Edin, F. Vecchi, M. C. Carrozza, and R. S. Johansson, "Humans Can Integrate Force Feedback to Toes in Their Sensorimotor Control of a Robotic Hand," *IEEE Trans. on Neural Systems and Rehab. Eng.*, vol. 17, no. 6, pp. 560–567, 2009.
- [7] J. L. Collinger, B. Wodlinger, J. E. Downey, W. Wang, E. C. Tyler-Kabara, D. J. Weber, A. J. C. McMorland, M. Velliste, M. L. Boninger, and A. B. Schwartz, "High-performance neuroprosthetic control by an individual with tetraplegia," *The Lancet*, vol. 381, no. 9866, pp. 557–564, 2013.
- [8] J. Tegin and J. Wikander, "Tactile sensing in intelligent robotic manipulation – a review," *Industrial Robot*, vol. 32, no. 1, pp. 64–70, 2005.
- [9] D. Alvares, L. Wiczorek, B. Raguse, F. Ladouceur, and N. H. Lovell, "An evaluation study of nanoparticle films as biomimetic tactile sensors," *Sensors and Actuators A: Physical*. Jun-2012.
- [10] D. Alvares, L. Wiczorek, B. Raguse, F. Ladouceur, and N. H. Lovell, "Development of nanoparticle film based multi-axial tactile sensors for biomedical applications," *Sensors and Actuators A: Physical*, in press.
- [11] R. S. Johansson and G. Westling, "Signals in tactile afferents from the fingers eliciting adaptive motor responses during precision grip," *Experimental Brain Research*, vol. 66, no. 1, pp. 141–154, 1987.
- [12] A. N. Burkitt, "A review of the integrate-and-fire neuron model: I. Homogeneous synaptic input.," *Biological Cybernetics*, vol. 95, no. 1, pp. 1–19, 2006.
- [13] J. Herrmann, K. H. Müller, T. Reda, G. R. Baxter, B. Raguse, G. J. J. B. De Groot, R. Chai, M. Roberts, and L. Wiczorek, "Nanoparticle films as sensitive strain gauges," *Applied Physics Letters*, vol. 91, no. 18, p. 183105, 2007.
- [14] K. F. Anderson, "The loop technique for strain gage rosette," *Experimental Techniques*, vol. 24, pp. 21–23, 2000.
- [15] I. Penskiy, a P. Gerratt, and S. Bergbreiter, "Friction, adhesion and wear properties of PDMS films on silicon sidewalls," *J. of Micromech. and Microengineering*, vol. 21, no. 10, p. 105013, 2011.
- [16] S. S. Kim, A. P. Sripathi, and S. J. Bensmaia, "Predicting the timing of spikes evoked by tactile stimulation of the hand.," *J. Neurophys.*, vol. 104, no. 3, pp. 1484–96, Sep. 2010.
- [17] J. Luo, K. Ying, P. He, and J. Bai, "Properties of Savitzky-Golay digital differentiators," *Digital Signal Processing*, vol. 15, no. 2, pp. 122–136, 2005.
- [18] S. S. Kim, S. Mihalas, A. Russell, Y. Dong, and S. J. Bensmaia, "Does afferent heterogeneity matter in conveying tactile feedback through peripheral nerve stimulation?," *IEEE trans. on Neural Systems and Rehab. Eng.*, vol. 19, no. 5, pp. 514–20, Oct. 2011.
- [19] L. Paninski, J. W. Pillow, and E. P. Simoncelli, "Maximum likelihood estimation of a stochastic integrate-and-fire neural encoding model.," *Neural Computation*, vol. 16, no. 12, pp. 2533–61, Dec. 2004.
- [20] I. Birznieks, H. E. Wheat, S. J. Redmond, L. M. Salo, N. H. Lovell, and A. W. Goodwin, "Encoding of tangential torque in responses of tactile afferent fibres innervating the fingerpad of the monkey," *J. Phys.*, vol. 588, no. Pt 7, pp. 1057–1072, 2010.